Geopersia ***10*** *(2), 2020, PP. 277-287* *DOI: 10.22059/GEOPE.2019.287542.648496*

Carbonate rocks microfacies analysis by using images processing and classification algorithms: an example from the Salman Oil and Gas field, Persian Gulf, Iran

Saeed Yarmohammadi[1], Ali Kadkhodaie[2]*
[1] *Petroleum Engineering Department, Petropars LTD Company, Tehran, Iran*
[2] *Department of Earth Sciences, Faculty of Natural Sciences, University of Tabriz, Tabriz, Iran*
**Corresponding author, e–mail: kadkhodaie_ali@tabrizu.ac.ir*
(*received: 19/08/2019 ; accepted: 22/12/2019*)

Abstract

Finding and quantifying microscopic features such as matrix and grains, fabrics, porosity, fossil contents and diagenesis are crucial to improving the results of a microfacies study. Moreover, the application of image processing seems essential in recognizing paleoenvironmental conditions and depositional setting analysis of hydrocarbon fields. There is a wide range of available image processing algorithms. However, these algorithms are dealing with many difficulties when faced with complex microfacies study objectives. In this paper, several thin section photographs from a Permo–Terias formation of Salman field in south–west of Iran were analyzed. Using the suggested histogram equalization algorithm, the selected thin section images were improved in a way to be comparable with the reference photographs. Afterward, the main microfacies major features such as matrix texture, boundaries, fossil content and appearance are characterized by applying functional image processing algorithms and sensitivity analysis of the algorithm results. Accurate grain size is measured in a designed Graphical User Interface (GUI). Next, pore detection and 2D porosity values are calculated by K–means clustering of A and B parameters in L*A*B image color space. Finally, different minerals in the matrix, cement, and porosity are classified and distribution of them are visualized and plotted on a scatter plot to determine the exact facies types.

Keywords: *Microfacies, Image Processing, Edge Detection, Gamma Correction, K–Means Clustering, K Nearest Neighboring Classifier.*

Introduction

There are a number of reasons for studying sedimentary rocks. It is worthy, not only because of economic minerals and materials contained within them but, hydrocarbon resources are driven from the maturation of organic matter in enriched sedimentary source rocks and migrate mostly into porous sedimentary reservoir rocks (Miall, 1990).

Sedimentological and petrological techniques are progressively used in the study of facies in depositional settings. These progresses lead petroleum geologists toward minimum uncertainties by finding modern solutions within image analysis methods. The image processing methods can make thin section studies quantitative and accentuate on important features (Tucker, 2001).

The carbonate formations are originated from primary dead organisms and carbonate chemical precipitations; so, they indicate a heterogeneous complex grain/pore systems (Choquette & Pray, 1970).

In the beginning, Microfacies was defined as the study of the thin section in terms of the petrographic and paleontological index.(Brown, 1943) and (Cuvillier, 1952). It is currently referred to all sedimentological and paleontological criteria which are received from the study of thin sections, peels, polished slabs or rock samples (Flügel, 2013).

Hence, most environmental interpretation of carbonate reservoirs is directly related to thin–section investigation with respect to microfacies concepts such as that Wilson (1975) conducted in lower Carboniferous Waulsortian facies (Wilson, 1975).

Image–processing techniques for rock features characterizing of thin sections are valuable and advantageous. The main advantage of this new techniques are time saving and accuracy of high–resolution analysis comparing with other conventional qualifying microscopic methods. The digital image analysis is also applicable for deriving mineral particle, fossil content, pore size characters and distribution, and digenesis effects (Seelos & Sirocko, 2005).

Visual description and classification of carbonate porosity were proposed by (Lucia, 1983), additionally, relationship between petrology of reservoirs such as pore geometry and petrophysical data was highlighted in other studies (Ehrlich *et al*.,

1984).

Thin section image clustering provides reliable data for 2D porosity values and Features geometry.

Considering these advantages, using K–mean clustering method in L*A*B, image spaces are proposed to calculate porosity by counting the number of specified color pixel and dividing it by the total number of image pixels.

K–means clustering is a simple implementation method for achieving decent results (Sidqi & Kakbra, 2014).

The K–nearest neighbor classifier is a conventional method for nonparametric classifying of data with optimal values of the classes (K). In the K – nearest neighbor classifying, the most frequent class accounts for a test sample. In the case of two or more same classes, the minimum average distance considers as the base of classifying (Kataria & Singh, 2013).

In the present study, the aforementioned concepts are used to enable sedimentologists to analysis the microfacies quantitatively and give them a clue to visualize segmented features in carbonate thin section images.

Geological setting

The Salman field was discovered in December 1965, with drilling and completion of a discovery well located in the Persian Gulf, Iran (Figure 1). Salt tectonics has a dominant influence in the formation of Salman field elliptical structure. According to many studies, Salman oil field was formed by Precambrian Hormoz salt movements (e.g. Stocklin, 1968; Kent, 1970; Nasir *et al*., 2008; Bruthans *et al*., 2010; Arian & Noroozpour, 2015; Perotti *et al*., 2016).

This field encountered three oil–bearing formations namely; Dariyan (U.A.E.: Shuaiba), Gadvan (UAE: Buwaib) and Surmeh (UAE: Arab), and two gas bearing formations namely Kangan–Dalan (UAE: Khuff), and Faraghan.

Oil–bearing reservoirs were deposited during Jurassic (Surmeh) and Cretaceous (Dariyan & Gadvan) time as result of sea level fluctuations in the Persian Gulf (Alsharhan & Nairn, 1989) and also rifting of Neo–Tethys Ocean (Stampfli & Borel, 2002).

In addition, detail study showed that Kangan and Dalan formations are compensated gas–bearing reservoirs. Kerogens of upper shale and intraformational carbonates are considered as source rock of .Kangan and Dalan formations.

The Khuff (Kangan/Dalan) formation was introduced in Steineke studies in 1937 (Powers, 1968) the studied type section is exposed in lowermost carbonate rock of Central Arabia (Al-Aswad, 1997).

The Kangan and Dalan formations are known as a complex reservoir in the Middle East. The complexity of carbonate can be attributed to variations in the depositional environment (Figure 2) in which they are formed and to extreme diagenesis.

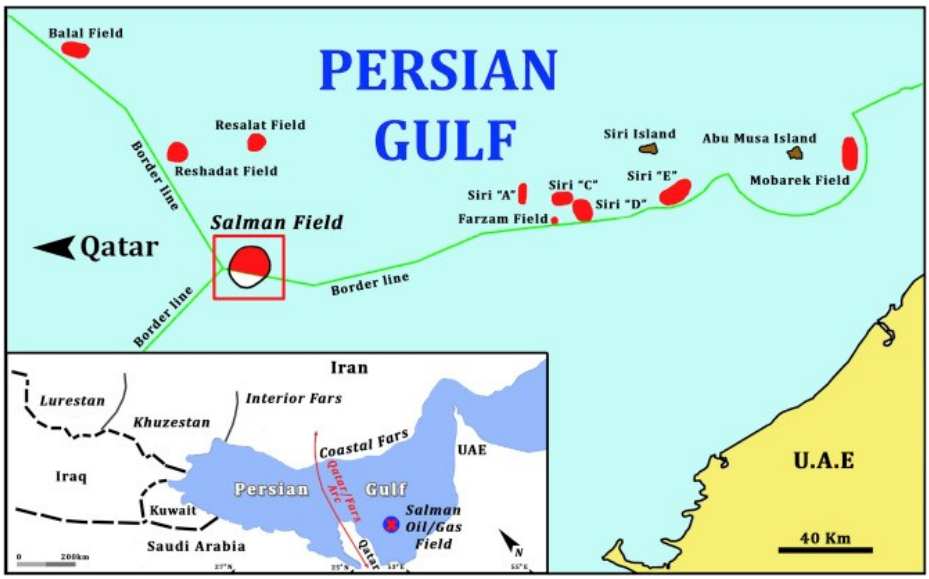

Figure 1. Location Map of Salman Field in the Persian Gulf (Beigi *et al*., 2017).

It is a cycle of carbonate–evaporate rocks deposited from Middle–Late Permian to early Triassic. Khuff's (Kangan/Dalan). Lithological changes are similar throughout the Persian Gulf including limestone, dolomite, anhydrite, and minor traces of shale. However, the Khuff (Kangan/Dalan) is often separated into an upper and lower unit by the widespread middle anhydrite layer called, Nar member (Szabo & Kheradpir, 1978).

Methodology

Image Preparing (Histogram Equalization)

A reliable image processing for categorizing of photos in different classes requires comparable average values in color spaces .i.e. RGB or L*A*B. Histogram Equalization is an image optimization method that changes image histogram and redistributes the pixels values to creates a color map close to possible to a user–specified desired histogram (Vij & Singh, 2011). Different features in a photo or two separated photos should be adjusted based on a user confirmed reference.

In microfacies study, for having a comparative thin section image analysis, some thin sections with desirable quality are selected as references. The references Red–Green–Blue (RGB) colors histograms are specified, afterward, a transformation could be applied to RGB colors of other photos using the Histogram Equalization technique (Figure 3). For different photos in different depths, histogram equalization need a transformation according to references photos. Accordingly the resultant images will be received comparability with their references (Figure 4).

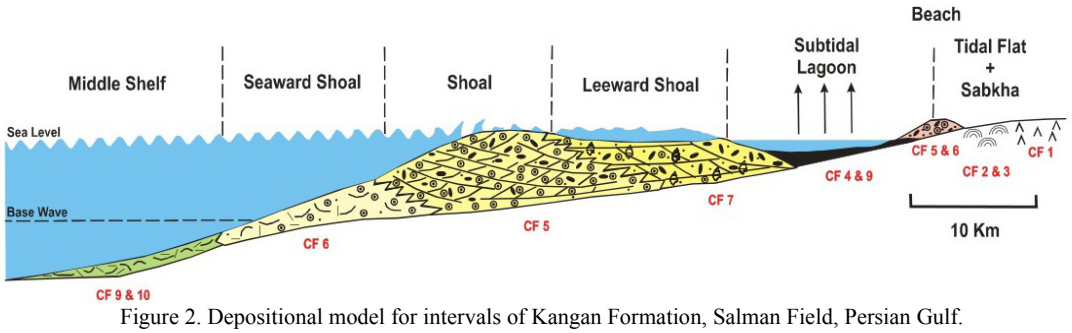

Figure 2. Depositional model for intervals of Kangan Formation, Salman Field, Persian Gulf.

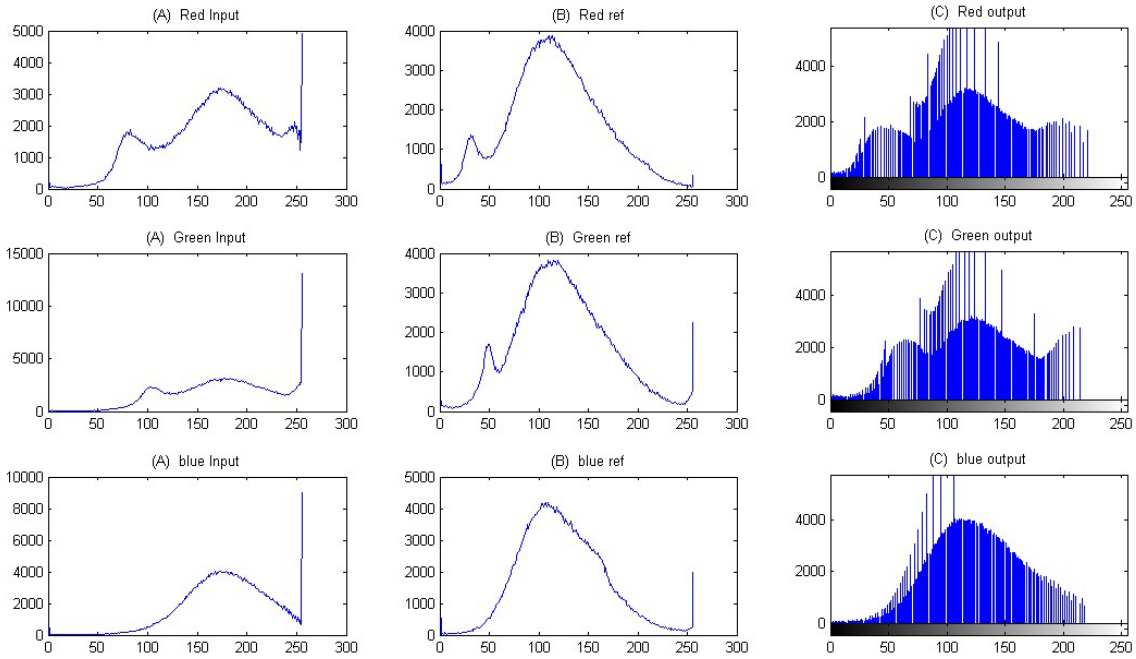

Figure 3. Equalization of input image RGB histogram (A) based on selected reference photo RGB histogram (B) output transformed RGB histogram (C).

Grain size

In microfacies, the grain size is the measurement of the longest diameter of 100 to 200 grains. Grain size variation may reflect changes in the depositional environment (Flügel, 2013).

A Graphical User Interface (GUI) in MATLAB is defined as a graphical display that enables the user to do interactive tasks by using designed components (windows containing controls) (Victoria *et al*., 2016).

In this study, a program was written in (GUI) environment to measure grain and pore sizes according to predefined microscopic scales. The program helps the user to open desired images from the browse tab. Then, the image scale is introduced by clicking on two end of a predefined microscopic scale. At the end, the obtained scale is considered as the base of features measurement within the section image (Figure 5).

Edge detection (features shapes and Boundaries)

In image processing, Edge detection methods are used to identify the edges and boundaries.

Edge in a photo is an image intensity change that makes a continuous curve. Edges are often referred to the boundaries of features in a thin section. Edge detection is a useful algorithm in the identification of fossil shapes and grain boundaries in an image.

In order to find the edges, edge function provides a number of first or second derivative estimators. For some of these estimators, sensitivity can be specified for a different direction of horizontal edges, vertical edges, or both (Maini & Aggarwal, 2009).

In the end, the edge would be distinguished in a binary image space. In this space, the edge pixel containing 1's while the other pixels have 0's values.

For a better understanding of textures in thin section and also the connection of grains and pores, edge detection methods are employed to sharpen them. Adjustable sensitive algorithms of edge detection method are provided to distinguish the grains/pores (Figure 6) and isolating them from the matrix (Figure 7).

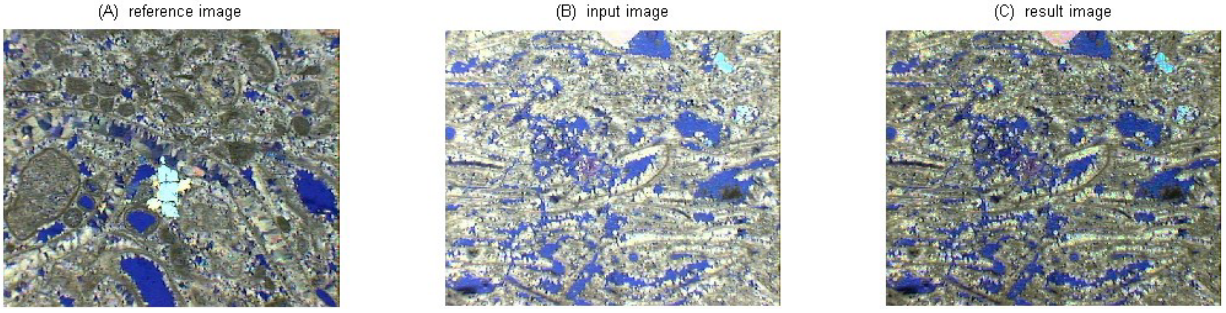

Figure 4. (A) Reference thin section image (Ooid, skeletal grainstone, Kangan formation, Depth=3622MD), (B) input thin section image (Ooid, skeletal grainstone, Kangan formation, Depth=3621MD), (C) result thin section image after applying histogram equalization.

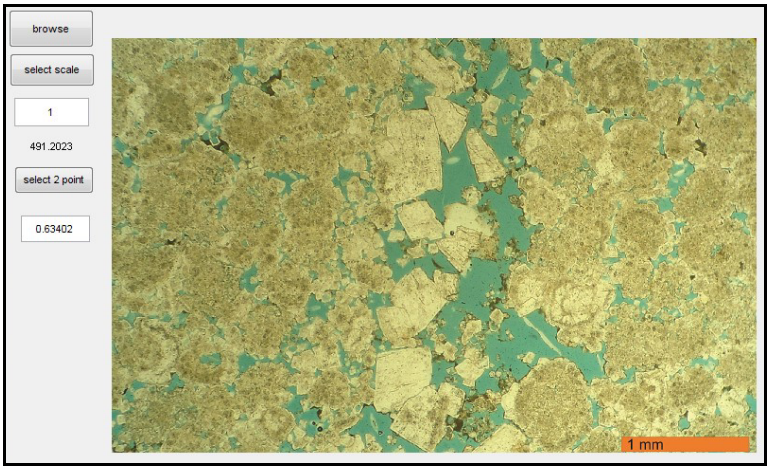

Figure 5. A snapshot of the designed graphical user interface for features measurements (Grains, pores) based on defined scale.

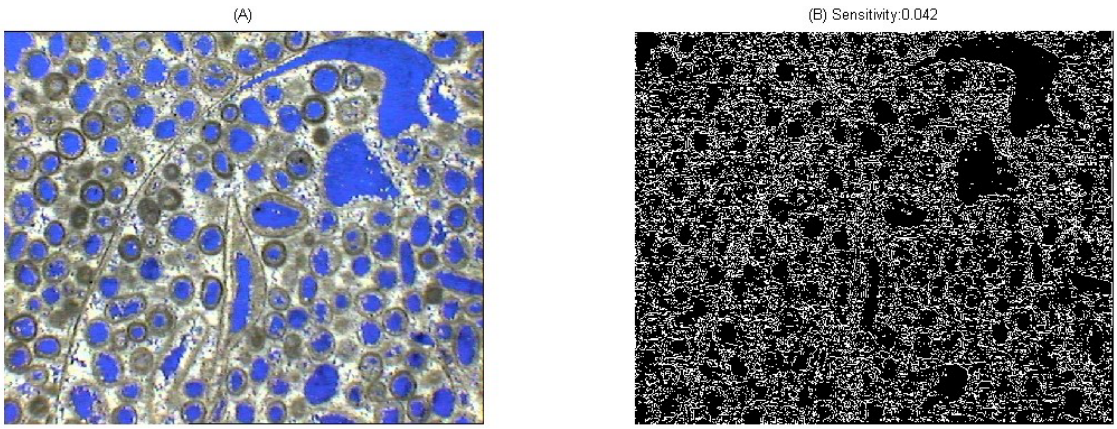

Figure 6. (A) Input thin section image (Skeletal, ooid grainstone with interparticle and oomoldic porosity, Kangan formation, Depth=3625) (B) Use of different edge detection method with different sensitivities to find best edge detection.

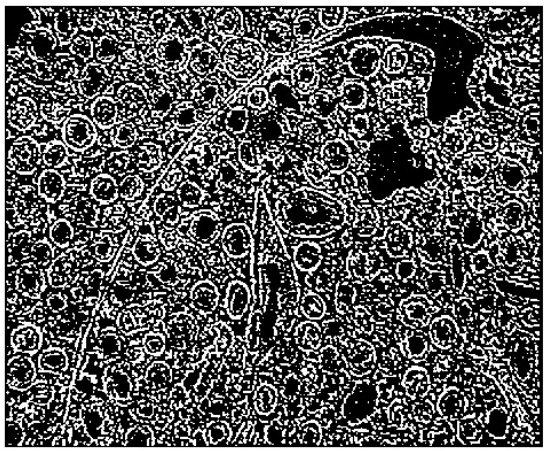

Figure 7. Output of the best edge detection on thin section image.

Image arithmetic operation for fossils analysis

Sometimes morphological and micro–structural diversity of skeletal grains are both ambiguous and variable. Moreover, distinguishing of important fossil groups in thin section provides an important data for interpretation of depositional processes.

In accordance with the complexity of identified fossil content, Image arithmetic operation could be applied to thin section photos. Image arithmetic is the enforcement of four basic mathematical operations including: addition, subtraction, multiplication, and division, images (Matlab2013b, 2013). Image arithmetic is a method that can illustrate the features in fossil image processing clearly. For example, image subtraction can be applied to detect the architecture of the skeletal grains. Fossilized body parts can also be figure out from back ground by complementing of a binary image. Complement algorithm reverses black and white colors in a binary image (Figure 8).

Gamma correction for birefringent minerals

Gamma correction function is used to correct the image's luminance– the brightness level of an image pixel –which is the average of RGB values. Gamma correction refers to the operation that encodes the linear luminance values into a non–linear relationship (Maurya & Magar, 2018).

In thin–section photomicrograph (cross–polarized light), cement and matrix have different mineral colors and birefringence. Birefringent minerals are optically anisotropic because their molecules do not respond to the incident light evenly in all directions (Hecht *et al*., 1998). Anhydrite crystals have high birefringence and also common sulfate and halide minerals are known as a birefringent mineral with the lower order (Scholle & Ulmer–Scholle, 2003). Extensive anhydrite cementation and replacement are effective diagenetic features in a carbonate formation. Anhydrite cement can be distinguished in a different form of blocky, lath–shaped, gypsum associated and etc… (Fu *et al*., 2002).

In this study, the Gamma correction function is

used to intensify colors in particular birefringent minerals in thin section images. Non–linear luminance which is achieved through gamma correction could guide us toward the clear distinction between birefringent minerals and cement such as anhydrite from most of the grains in deposits (Figure 9).

K–means clustering (2D porosity values and pore geometry)

Cluster analysis gathers objects into different groups by considering objects data and their relationships (Tan *et al*., 2013).

K–means is a method of clustering, in this method clustering objects groups into a specific number of separated clusters. In these methods, K refers to the Number of clusters. There is a different function of distance measurements that determine which object can be appended to which cluster. The method is very effective in minimizing the measurement between the centroid of the clusters and objects. Iteration appends an object to any cluster when the minimum distance measure is achieved. Basically, distance measurement is defined as $D(x,y) = \|x^2 - y^2\|$ (Euclidean distance) to determine a type of category for an object in terms of different clusters (Burney & Tariq, 2014).

Each pixel in an image has certain features according to which it could be clustered with others. L*A*B color space is a color–special space in which L is a dimension for lightness and A and B for the color (Sidqi & Kakbra, 2014).

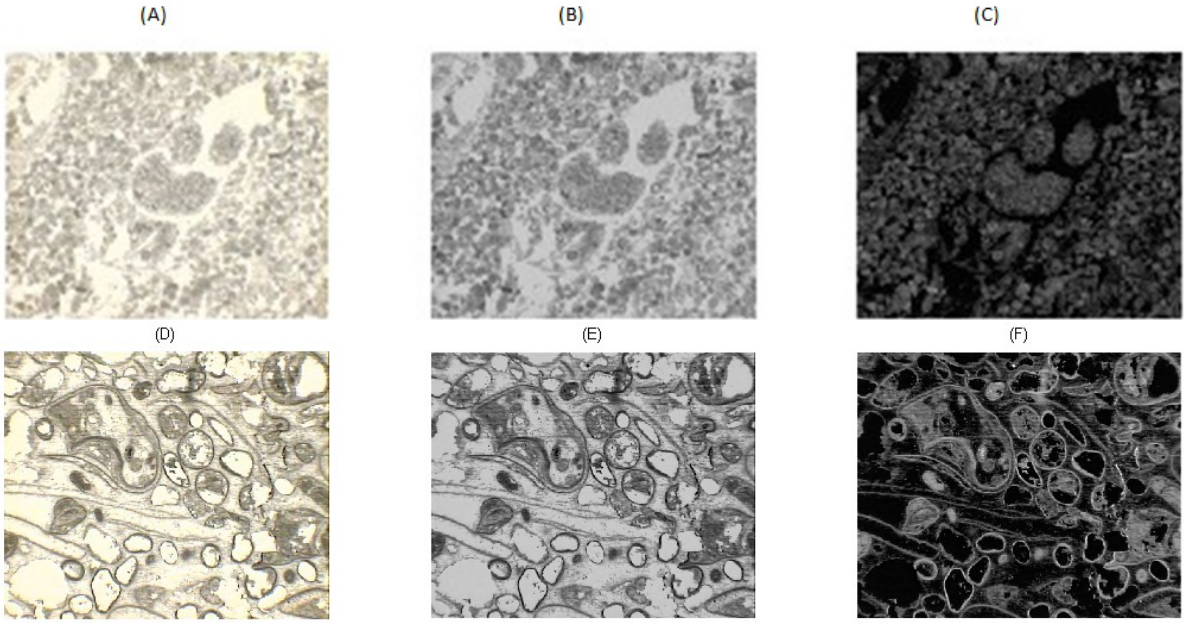

Figure 8. (A) thin section image of a Gastropod fossil (Depth=3633.32); (B) subtraction image of original image (A); (C)complement image of original image (A); (D) thin section image of a fossil (Gastropod) from the other side (Depth= 3622.82); (E) subtraction image of original image (D); (F) complement image of original image (D).

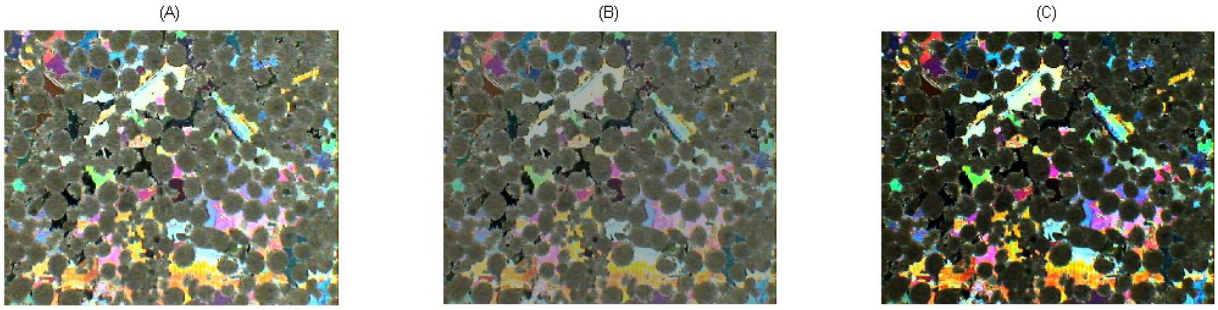

Figure 9. (A) Original thin section image with Anhydrite cement (Peloid, Ooid dolograinstone with secondary anhydrite cement, Kangan formation, Depth=3696.19); (B) Highlighted grains (Oolite) using De–gamma correction; (C) Highlighted Anhydrite cementation using gamma correction.

In the present study, 2D porosity values and pore geometries were estimated using the K–means clustering method. For this reason, first RGB thin section images are transferred to L–A–B color space.

In L–A–B color space, two components of A and B are clustered by K–mean methods. Two centroids were defined in which porosity in thin section images has specified color (Dark–blue) and other features could be grouped in another cluster. 2D porosity values are calculated from the ratio of porosity color pixels to total counted pixels of the image. Furthermore, the geometry of pores in the clustered image are clearly segmented for pore type analysis (Figure 10).

Nearest neighbor classifiers for thin section features segmentation

In carbonate thin section images, there are a number of elemental features including grains, cement, fossils, and porosities that need to be classified and their ratio to be investigated. Accordingly, it is considered that image segmentation and classifying is a fundamental concept in the thin section image study.

In this study, an image segmentation method, using nearest neighbors' classifier, is used to formulate carbonate thin section images into discrete microfacies.

Nearest Neighbors (kNN) is based on similar features. This algorithm is a new method that separated a defined database into several classes to predict the classification of new data points. (Sutton, 2012).

For thin section images, the regions of pixels are marked to a set of rock features (minerals or pores) in which case the precise classification of an algorithm is defined. Therefore, training sets for the algorithm are constructed and nearest neighbor classifier predicts the decision boundaries for given regions in thin section images as the training set (Table 2) (Figure 11).

Finally, the thin section segmented into several identified regions with specified color and their ratio visualized on a cross plot (Figure 12).

The classified colors which are indicators of microfacies features (grains and pores) make the evaluation comparable and classified.

Discussion

In order to have determined study, in this essay, core data (Three intervals, totally about 100m) from Kangan formation of a well type in Salman field was chosen. Core study result shows that Kangan formation includes 10 facies. They are named as CF1 (Anhydrite), CF 2 (Dolomitic or lime mudstone fabric, mud cracks and evaporate pore filling), CF 3 (Laminated stromatolite boundstone often with evaporatic fenesteral dolomudstone), CF 4 (Lagoonal skeletal, peloid, encode, intraclast wackestone / packstone), CF 5 (Medium–grained laminated and cross bedded ooid grainstone), CF 6 (Coarse–grained skeletal, intraclast grainstone / packstone along with coarsening upward cycle and oncoid debris), CF 7 (Fine to medium–grained ooid, peloid grainstone / packstone), CF 8 (Intraformational conglomerate with fining upward cycle), CF 9 (Bioturbated peloidal mudstone to peloid, skeletal wackestone, and CF 10 (Dark laminated open marine fossiliferous mudstone) respectively **Error! Reference source not found.** (Figure 2). Then, several thin section photos were selected as samples for image processing and different image processing functions in particular clustering and classifying methods provided interesting approach for carbonate microfacies studies.

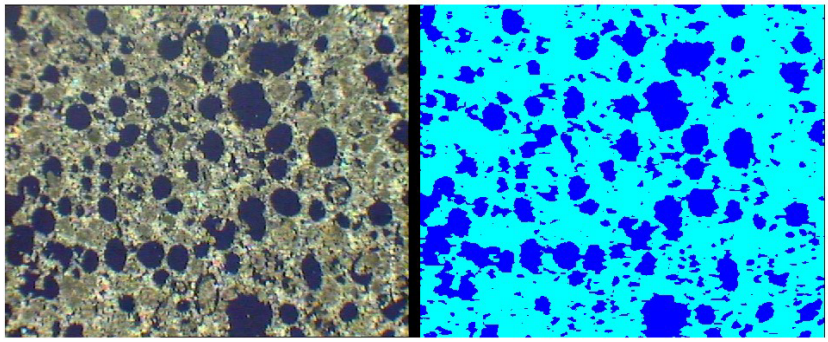

Figure 10. K–means clustered thin section image to calculate 2D porosity values and pore geometry (Ooid grainstone with oomoldic porosity,Kangan formation, Depth=3670MD), The thin section image dimensions is 704*576 pixels, Vertical and horizontal resolution are 300dpi, 2D porosity=29%.

Table 1. Statistical parameters of porosity and permeability distributions in various core facies.

Core Facies	n	Helium Porosity (%)				Air Permeability (mD)			
		Max.	Mean	Min.	Std. Dev.	Max.	Mean	Min.	Std. Dev.
CF1	2	1.10	0.65	0.20	0.64	0.574	0.292	0.009	0.400
CF2	41	30.00	10.26	0.50	7.34	511.000	43.518	0.001	95.798
CF3	5	12.40	7.52	1.10	4.09	13.699	3.753	0.009	5.962
CF4	18	27.30	11.03	0.90	8.02	237.000	41.517	0.024	76.652
CF5	55	28.70	11.69	0.70	7.25	1290.000	77.896	0.002	233.508
CF6	38	24.50	11.28	1.00	7.72	159.000	27.948	0.004	42.760
CF7	49	27.50	10.33	0.80	6.90	2093.448	113.298	0.002	326.712
CF8	0	–	–	–	–	–	–	–	–
CF9	5	11.40	4.48	0.60	4.68	12.600	4.274	0.001	5.175
CF10	8	6.30	4.16	1.10	1.97	9.636	1.614	0.003	3.321

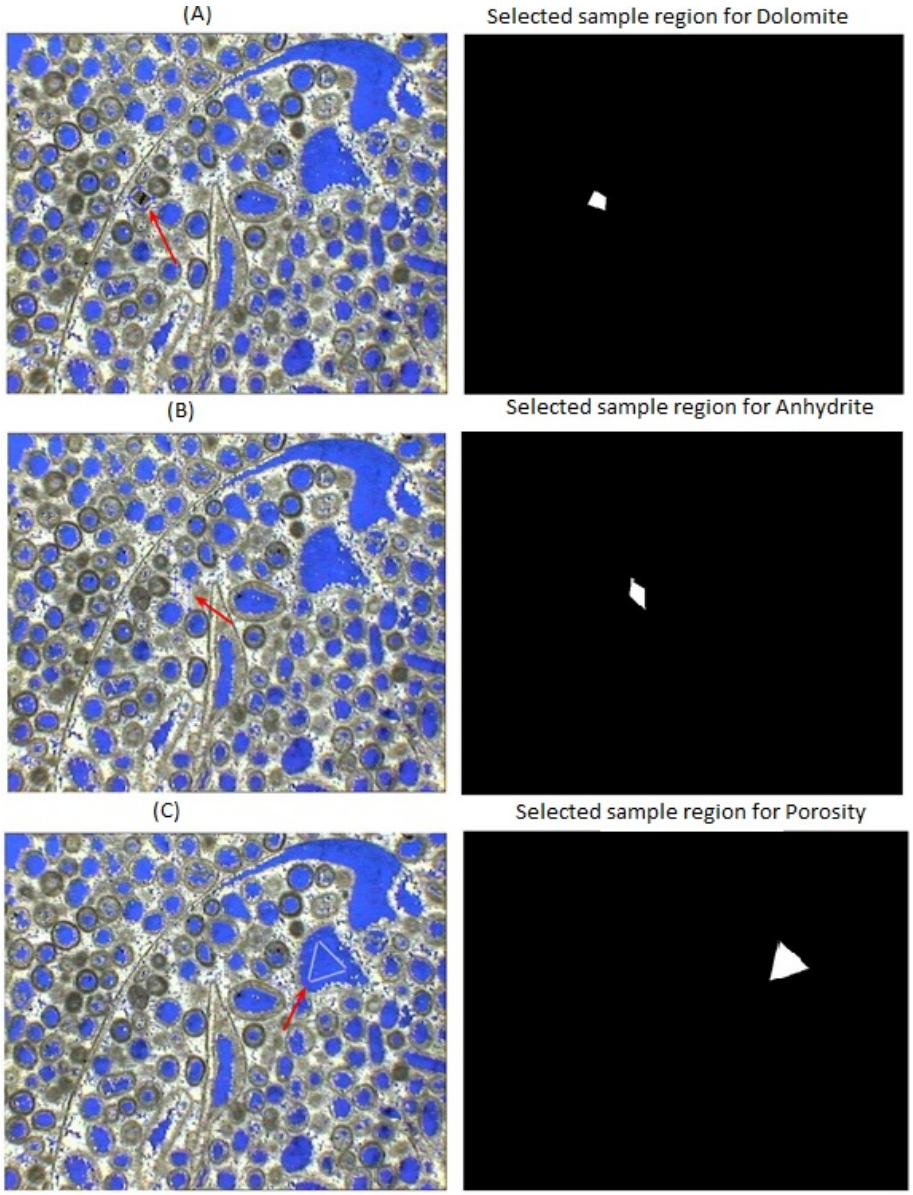

Figure 11. (A) selected region for classifying of dolomitic grains; (Oolites) (B) selected region for classifying of Anhydrite cementation; (C) selected region for classifying of porosity.

Table 2. Average of Image color values in RGB and L*A*B color spaces for selected regions in thin section.

Features	RGB color space			L*A*B color space		
	Ave_Red	Ave_Green	Ave_Blue	Ave_L	Ave_A	Ave_B
anhydrite	210.23	215.78	206.51	217.83	124.84	131.90
Ooid	51.77	87.99	236.50	103.01	125.51	133.36
porosity	94.05	96.46	86.51	108.55	157.65	47.97

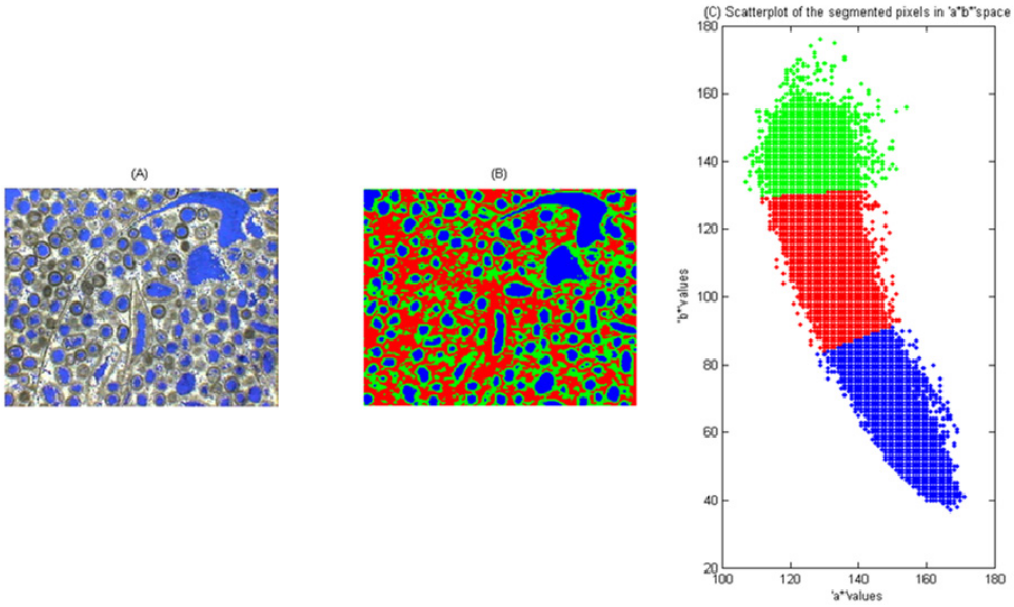

Figure 12. (A) original thin section image (B) Features (Grains (Oolite), Cement (Anhydrite), Porosity) segmented thin section image by using K nearest neighbor classifier (C) Scatter plot of the segmented pixel in L*A*B space for defining of features ratios.

Comparative images were received through histogram equalization algorithms based on choosing a high–quality reference image (Figure 3 & Figure 4). Appropriate pore /grain size measurements were determined using a Graphical User Interface (GUI) in MATLAB (Figure 5Figure 4). Thin section features were investigated trough edge detection methods and they were optimized by different sensitivities (Figure 6 & Figure 7). Image arithmetic operations were used to clarify the fossil types (Gastropods) in Kangan depositional system. Two thin sections with the same fossil content from a plug can have different appearances (Figure 8). This is due to the preparation of thin sections from two different sides. Determination of cement types is necessary for the interpretation of the carbonate reservoirs. For example, development of a small amount of anhydrite cement on pore throats of a peloid dolograinstone causes a severe reduction of porosity and permeability. Based on interpretation of Kangan formation sedimentary environment, Gamma correction was applied on thin section images to magnify image luminescence and highlight birefringent anhydrite cementation (Figure 9).

In the next step, an attempt is made to quantify images in terms of 2D porosity values and geometry using K–means clustering. Thin section images of Salman field were transferred from RGB to L*A*B color space and porosity values were extracted using clustering of A and B parameters (Figure 10).

Accurate microfacies were distinguished through image segmentation based on nearest neighbors classifying and finding the ratio of features Table 2 (Figure 11 & Figure 12).

Image processing results demonstrated that use of image processing methods in several step could decrease the uncertainties in microfacies interpretations of carbonate reservoirs and quantitative results show an outstanding adaptation with common microscopic studies.

Conclusion

In this paper, image processing approaches were proposed for thin section study of carbonate microfacies. Integration of different image processing algorithms, image K–mean clustering and nearest neighbor classifying demonstrated that image

processing can be considered as an effective tool in the microfacies study of carbonate rocks. The histogram equalization method made the thin section images comparative. Grain size as fundamental features of a thin section was measured precisely in the GUI environment. Grains–pores boundaries were successfully isolated by using edge detection methods and its accuracy was optimized by sensitivity analysis. Fossil contents were investigated morphologically in different Image arithmetic operations. Quantified 2D porosity was calculated using the K–mean clustering of thin section images in L*A*B spaces. Moreover, highlighted pore geometry in clustered images was introduced for better reservoir characterizations. In the end, an image nearest neighbor classifier shows that different features of carbonate thin sections include (grain mineral, cementation, fossils, and pores) can be segmented in different classes and their ratio lead interpreter toward a better understanding of depositional settings and environments.

Acknowledgments

Vice–Chancellor for Research and Technology of the University of Tabriz is acknowledged for preparing financial support to carry out this research (Grant No. 822).

References

Al-Aswad, A., 1997. Stratigraphy, sedimentary environment and depositional evolution of the Khuff Formation in south-central Saudi Arabia. Journal of Petroleum Geology, 20: 307–326.

Alsharhan, A., Nairn, A., 1989. Sedimentary basins and petroleum geology of the Middle East. A publication of elsevier, 843p.

Arian, M., Noroozpour, H., 2015. Tectonic geomorphology of Iran's salt structures. Open Journal of Geology, 5: 61.

Brown, J. S., 1943. Suggested use of the word microfacies. Economic Geology, 38: 325.

Bruthans, J., Filippi, M., Zare, M., Churáčková, Z., Asadi, N., Fuchs, M., Adamovič, J., 2010. Evolution of salt diapir and karst morphology during the last glacial cycle: effects of sea–level oscillation, diapir and regional uplift, and erosion (Persian Gulf, Iran). Geomorphology, 121: 291–304.

Burney, S. A.,Tariq, H., 2014. K–means cluster analysis for image segmentation. International Journal of Computer Applications, 96.

Choquette, P. W., PRAY, L. C., 1970. Geologic nomenclature and classification of porosity in sedimentary carbonates. AAPG bulletin, 54: 207–250.

Cuvillier, J., 1952. La notion de" microfaciès" et ses applications. VII Convegno nationale del Metano et del Petrolio, Prestampa, Sezione I: 3–7.

Ehrlich, R., Kennedy, S. K., Crabtree, S. J., Cannon, R. L., 1984. Petrographic image analysis; I, Analysis of reservoir pore complexes. Journal of Sedimentary Research 54: 1365–1378.

Flügel, E., 2013. Microfacies of carbonate rocks: analysis, interpretation and application, Springer Science & Business Media.

Fu, Q., Qing, H., Bergman, K., 2002. Petrography of diagenetic anhydrite in the Middle Devonian Winnipegosis and Ratner formations, south–central Saskatchewan. Summary of Investigations, Saskatchewan Geological Survey, 15–23.

Hecht, E., Zając, A., Guardino, K., 1998. Optics, Addison–Wesley.

Kataria, A., Singh, M., 2013. A review of data classification using k–nearest neighbour algorithm. International Journal of Emerging Technology and Advanced Engineering, 3: 54–360.

KENT, P., 1970. The salt plugs of the Persian Gulf region. Transactions of the Leicester Literary and Philosophical Society, 64.

Lucia, F., 1983. Petrophysical parameters estimated from visual descriptions of carbonate rocks: a field classification of carbonate pore space. Journal of petroleum technology, 35: 629–637.

Maini, R. & Aggarwal, H., 2009. Study and comparison of various image edge detection techniques. International journal of image processing (IJIP), 3: 1–11.

Matlab 2013B 2013. The MathWork, Natick.

Maurya, S. R., Magar, G. M., 2018. Impact of Gamma Correction on Quality of Geospatial 3D Reconstructions though Photogrammetry. International Journal of Scientific Research in Computer Science, 1: 1609–1616.

Miall, A. D., 1990. Principles of sedimentary basin analysis, Springer–Verlag.

Nasir, S., Al–Saad, H., Alsayigh, A., Weidlich, O., 2008. Geology and petrology of the Hormuz dolomite, Infra–Cambrian: Implications for the formation of the salt–cored Halul and Shraouh islands, Offshore, State of Qatar. Journal of Asian Earth Sciences, 33: 353–365.

Perotti, C., Chiariotti, L., Bresciani, I., Cattaneo, L., Toscani, G. 2016., Evolution and timing of salt diapirism in the Iranian sector of the Persian Gulf. Tectonophysics, 679: 180–198.

Powers, R., 1968. Saudi Arabia (excluding Arabian Shield), Centre national de la recherche scientifique.

Scholle, P. A., Ulmer–Scholle, D. S., 2003. A Color Guide to the Petrography of Carbonate Rocks: Grains, Textures, Porosity, Diagenesis, AAPG Memoir, 77, AAPG.

Seelos, K., Sirocko, F., 2005. RADIUS–rapid particle analysis of digital images by ultra-high-resolution scanning of thin sections. Sedimentology, 52: 669–681.

Sidqi, H. M., Kakbra, J. F., 2014. Image Classification Using K–mean Algorithm. International Journal of Emerging Trends & Technology in Computer Science (IJETTCS), 3: 38–41.

Stampfli, G. M., Borel, G., 2002. A plate tectonic model for the Paleozoic and Mesozoic constrained by dynamic plate boundaries and restored synthetic oceanic isochrons. Earth and Planetary Science Letters, 196: 17–33.

Stocklin, J., 1968. Structural history and tectonics of Iran: a review. AAPG Bulletin, 52: 1229–1258.

Sutton, O., 2012. Introduction to k nearest neighbour classification and condensed nearest neighbour data reduction. University lectures, University of Leicester, 1.

Szabo, F., Kheradpir, A., 1978. Permian and Triassic stratigraphy, Zagros basin, south-west Iran. Journal of Petroleum Geology, 1: 57–82.

Tan, P.–N., Steinbach, M., Kumar, V., 2013. Data mining cluster analysis: basic concepts and algorithms. Introduction to data mining. Pearson Addison–Wesley.

Tucker, M. E., 2001. Sedimentary Petrology: An Introduction to the Origin of Sedimentary Rocks, Wiley.

Victoria, M., Querin, O. M., Díaz, C., Martí, P. 2016. Liteitd A Matlab Graphical User Interface (GUI) program for topology design of continuum structures. Advances in Engineering Software, 100: 126–147.

Vij, K., Singh, Y., 2011. Enhancement Of Images Using Histogram Processing Techniques. Int. J. Comput. Technol. Appl, 2: 309–313.

Wilson, J. L., 1975. The Lower Carboniferous Waulsortian facies. Carbonate Facies in Geologic History. Springer.